ELSEVIER

Journal of Magnetism and Magnetic Materials 209 (2000) 220–223

Journal of magnetism and magnetic materials

www.elsevier.com/locate/jmmm

Geometric shape dependence of coercivity for patterned magnetic thin films

Te-Ho Wu[a,*], J.C. Wu[b], C.S. Wu[b], Bing-Mau Chen[c], Han-Ping D. Shieh[c]

[a]*Department of Humanities and Sciences, National Yunlin University of Science and Technology, Touliu 640, Taiwan, ROC*
[b]*Department of Physics, National Changhua University of Education, Changhua 500, Taiwan, ROC*
[c]*Institute of Electro-Optic Engineering, National Chiao-tung University, Hsinchu 300, Taiwan, ROC*

Abstract

The micro-strips with patterned magnetic domains using electron beam lithography have been made to study the geometric shape dependence of coercivity. The size of the micro-strip is 10 μm × 30 μm with 0.5 μm periods hole arrays pattern. Arrays with different types of geometry, such as square-, circle-, and ellipse-shapes have been made. Amorphous rear-earth transition-metal (RE-TM) thin films with magnetic perpendicular anisotropy were deposited on the micro-strips. The extraordinary Hall effect has been employed to measure the hysteresis loop and the coercivity of the sample. We have found that for the same deposited material, the magnitude of coercivity for various shapes are dissimilar. For example, the coercivity of the ellipse-shaped hole arrays is much larger than the coercivity of the square-shaped hole arrays. In addition, we observed that the coercivity of the patterned sites was larger than the sites without patterns for RE-dominated compounds and the coercivity of the patterned sites was smaller than the sites without patterns for TM-dominated compounds. The magnetic moments canting between RE and TM subnetworks will be used to explain the observed phenomena.

Keywords: Coercivity; E-beam lithography; Micro-structure; Shaped-dependence; Canting

1. Introduction

A major concern usually encountered in descriptions of the magneto-optical write and erase processes is the coercivity of the thin film material. Technically, the coercivity H_c is defined as for a hysteresis loop as the value of applied field at which the net magnetization becomes zero. Coercivity, however, is an ill-defined concept which may be useful in the phenomenology of bulk reversal, but its relevance to the phenomena occurring on the spatial and temporal scales of thermomagnetic recording must be seriously questioned. To begin with, there is the problem of distinguishing the nucleation coercivity from the coercivity of wall motion. Then there is the question of speed and uniformity of motion as the wall expands beyond the site of its origination. Finally one must address issues of stability and erasability, which are intimately related to coercivity, in a framework wide enough to allow the consideration of local instabilities and partial erasure. It is fair to say that the existing theories of coercivity [1–3] are generally incapable of handling the problems associated with magneto-optical recording and erasure. We have shown in previous publications that the patterned magnetic films possess different coercivity compared with films without patterns [4,5]. In addition, the various shapes of the patterned hole arrays also displayed different coercivity. In our view, the direct vehicle for conducting the coercivity investigations is via experimental methods. Thus, it inspired us to use micro-strip structures with different geometric hole arrays to explore the origins of coercivity.

2. The experimental methodology

Several magnetic micro-strips with various geometric hole arrays have been made. The fabrication procedures

* Corresponding author. Tel.: 886-5-534-2601 ext. 3166; fax: 886-5342601 ext. 3166.
E-mail address: wuth@flame.yuntech.edu.tw (T.-H. Wu)

0304-8853/00/$ - see front matter
PII: S0304-8853(99)00693-9

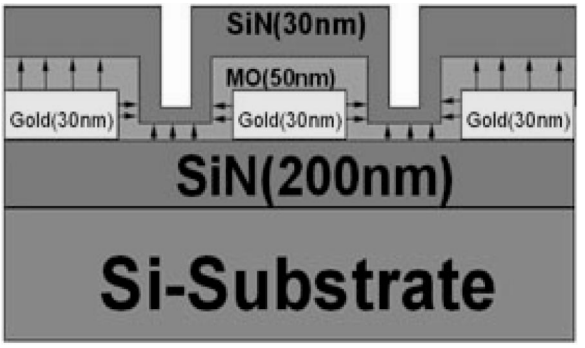

Fig. 1. Cross-sectional view of fabricated layer structure: silicon/SiN(200 nm)/DyFeCo(50 nm)/SiN(30 nm) in the holes and silicon/SiN(200 nm)/Au(30 nm)/DyFeCo(50 nm)/SiN(30 nm) otherwise on the gold ridges.

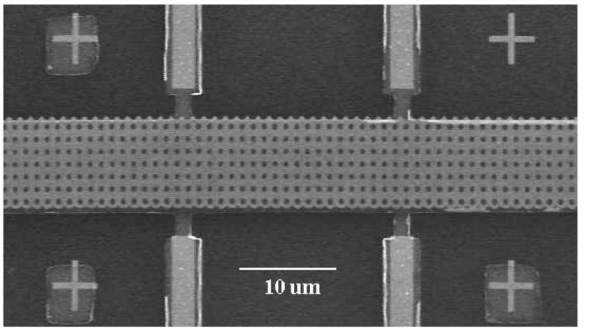

Fig. 2. An image taken from SEM; the magnetic micro-strip with artificial pinning sites for the square-shaped hole array image taken from SEM.

of these magnetic devices with artificial pinning sites are described as follows. A 10 μm wide gold strip with various geometric holes arrays were first fabricated on a Si_3N_4-coated silicon substrate by a lift-off process using electron beam lithography. The thickness of the gold strips is 30 nm. The square-, circle-, and ellipse-shaped hole arrays with a lateral dimension of 0.5 μm and a periodicity of 1 μm were produced along the gold strips. The elliptical holes have 1.0 μm on long axis and 0.5 μm along short axis. A second step of electron beam lithography was employed for making a long trench in the electron resist, in which the trench covered the gold strip. This process is necessary for the further lift-off procedure, after the magnetic film deposition, to take away the area without patterns to make the magnetic micro-strip. Trenches for the current and voltage leads were made at this time as well. The MO active layer DyFeCo with a thickness of 50 nm was then DC magnetron co-sputtered onto the pre-formatted pinning patterns, and a 30 nm thickness of SiN layer was subsequently deposited to protect the MO layer. In order to make the magnetic micro-strip a second lift-off process was performed to remove the area without any patterns. The final layer structures is shown in Fig. 1. The magnetic micro-strip with artificial pinning sites for the square-shaped hole array image taken from SEM is displayed in Fig. 2. An external magnetic field perpendicular to the film plane is applied and the extraordinary Hall effect has been employed to measure the hysteresis loop and the coercivity.

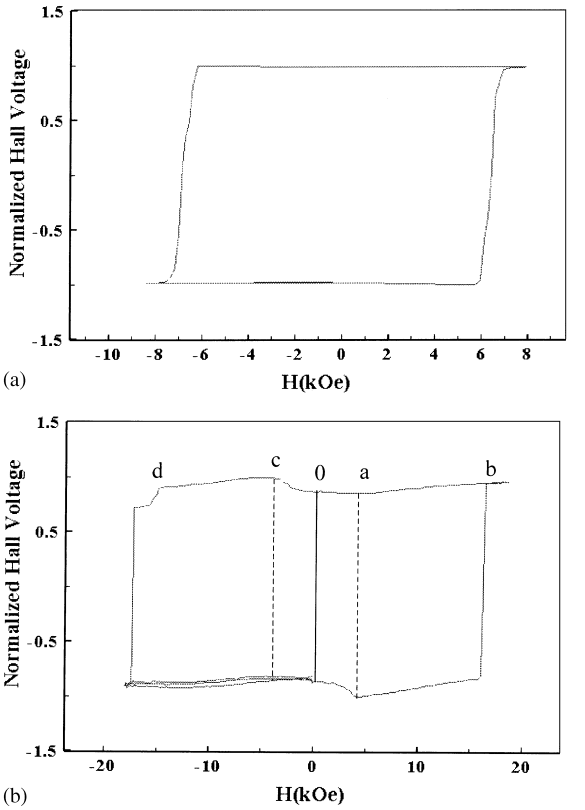

Fig. 3. Shows two V–H hysteresis measurements for sample $Dy_{26.9}(Fe_{80}Co_{20})_{73.1}$: (a) the film without patterned hole arrays; (b) ellipse-shaped pattern.

3. Results and discussions

Fig. 3 shows two V–H (Hall voltage versus external applied field) hysteresis loops for film $Dy_{26.9}(Fe_{80}Co_{20})_{73.1}$. The film without pattern is shown in Fig. 3(a) and the film with ellipse-shaped pattern (with long axis 1.0 μm and short axis 0.5 μm) is displayed in Fig. 3(b). The shape of the hysteresis loops (not shown) of the film with square- and circle-shaped are similar to Fig. 3(b). Table 1 summaries coercivity values versus different geometric shapes for various compounds of

Table 1
Coercivity values versus different geometric shapes for various compounds of $Dy_x(FeCo)_{1-x}$

Sample	$Dy_{26.9}(Fe_{80}Co_{20})_{73.1}$				$Dy_{21.0}(Fe_{80}Co_{20})_{79.0}$				$Dy_{22.3}(Fe_{80}Co_{20})_{77.3}$		
	RE-rich				TM-rich				TM-rich		
Shape	Ellipse	Circle	Square	No pattern	Ellipse	Circle	Square	No pattern	Ellipse	Square	No pattern
H_c (kOe)	16.78	14.77	12.55	6.88	1.37	1.53	0.23	2.51	3.54	3.51	5.5

$Dy_x(FeCo)_{1-x}$. We found that coercivity was enhanced the most for a RE-rich film with ellipse-shaped patterns. Among various patterned geometric shapes, the magnitude of coercivity in sequence is H_c (ellipse) $> H_c$ (circle) $> H_c$ (square); and the coercivity for a film without any pattern gave the smallest value. In addition, the hysteresis loop for thin film without pattern shows good squareness (see Fig. 3(a)), while for the patterned microstrips, the scheme of hysteresis loops are quite different; curvatures on both top and bottom parts of the loop have been observed, as shown in Fig. 3(b). The hysteresis behaviors of Fig. 3(b) is described subsequently. When the applied field was increased positively the Hall signal decreased first (points o to a), then increased linearly until the applied field ended (points a to b). Special attention should be paid when the applied field is reversed; the Hall signal increases and reaches to a maximum value (points o to c), then decreases monotonously until the magnetization reversal process begins (points c to d). The reasons for the aforementioned phenomena were due to three facts. The first cause was because of the presence of canting between RE and TM sub magnetic components [6]; the second reason was that the contributed EHE signal mainly comes from the TM sub magnetic component [7]; and the third reason was due to the existence of magnetic moments perpendicular to the side-wall around the hole arrays. A detailed theoretical model will be published on another paper.

The magnetic moment canting behavior also contributed to the coercivity sequence of H_c (ellipse) $> H_c$ (circle) $> H_c$ (square) $> H_c$ (without pattern). The reason for the patterned thin films possessing larger coercivity is due to the magnetization reversal processes being impeded by two coercive forces, one from the nucleation coercive force, and the other from the anisotropy coercive force. Due to the large canting angle, the anisotropy coercive force will impede the magnetization reversal process, thus increasing the coercivity value. This explains that the coercivity of the patterned films is larger than the film without pattern. Moreover, the reason for the ellipse-shaped pattern coercivity being larger than the circle- and square-shaped is as follows. For ellipse-shaped geometry, when the applied field pushes the canting angle on the short axis (the same radius as that of the circle-shaped hole) reaching the maximum angle θ_c, the canting angle of the long axis still has not reached θ_c. Thus, more external applied field is needed to reverse the magnetic moments to the other direction compared to the circle- and square-shaped patterns. As a result, the coercivity of the ellipse shape is larger than the circle and square shapes.

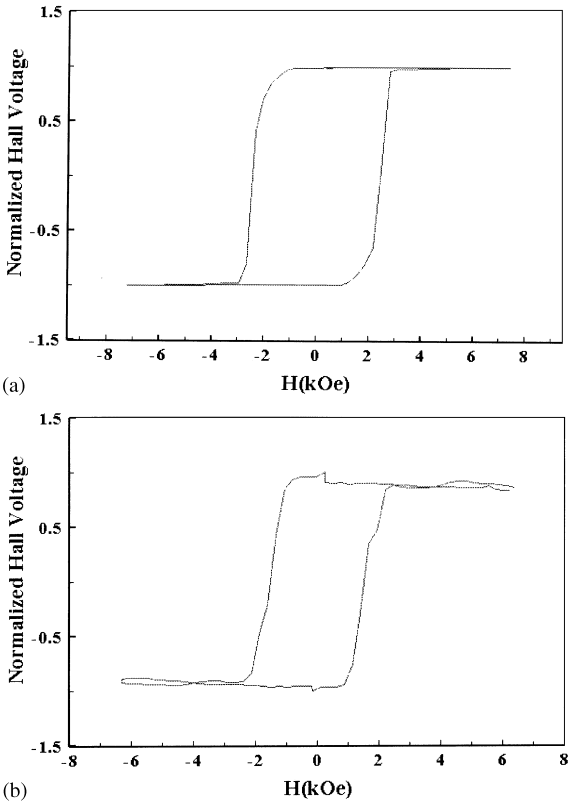

Fig. 4. Shows two V–H hysteresis measurements for sample $Dy_{21.0}(Fe_{80}Co_{20})_{79.0}$: (a) the film without patterned hole array; (b) ellipse-shaped pattern.

Fig. 4 shows two V–H hysteresis measurements for sample $Dy_{21.0}(Fe_{80}Co_{20})_{79.0}$. The film without patterned hole arrays is shown in Fig. 4(a) and the film with ellipse-shaped pattern (with long axis 1.0 μm and short

axis 0.5 μm) is displayed in Fig. 4(b). For TM-rich samples, however, the situations are much different from the RE-rich sample. As summarized in Table 1, the coercivity for a film without any pattern gives the largest value for samples $Dy_{21.0}(Fe_{80}Co_{20})_{79.0}$ and $Dy_{22.3}(Fe_{80}Co_{20})_{77.7}$. In addition, film with compound near compensation composition shows that the ellipse-shaped pattern has comparable coercivity with the square-shaped pattern. Moreover, the schemes of hysteresis loops, unlike the Dy-rich thin film, show better flatness on both top and bottom curves. These results could also be explained by the previously mentioned three facts. We conjecture that the reason that the hysteresis loops shows better flatness might be due to the exchange coupling strength and anisotropy energy, for $Dy_{21.0}(Fe_{80}Co_{20})_{79.0}$ sample is larger compared with Dy-rich sample [8]. As a result, the canting behavior of side-wall moments of the hole is not apparent. Thus, the hysteresis loops show flatness.

4. Concluding remarks

We have made a series of RE–TM amorphous microstrip samples to study the relationships among different geometric shapes, compounds of film, and coercivity. We have found that, for RE-rich samples, among various geometric patterned shapes the magnitude of coercivity in sequence is H_c (ellipse) $> H_c$ (circle) $> H_c$ (square) $> H_c$ (without pattern). For TM-rich samples, however, the situations are quite different. The coercivity for a film without any pattern gives the largest value and film with compound near compensation composition shows that the patterned ellipse-shape has comparable coercivity with the patterned square-shape. All the aforementioned phenomena can be explained by the magnetic moment canting behaviors between RE and TM subnetworks.

Acknowledgements

This work is supported by the National Science Council, the Republic of China, under contract No. NSC 88-2112-M-224-001.

References

[1] R. Friedberg, D.I. Paul, Phys. Rev. Lett. 34 (1975) 1234.
[2] D.I. Paul, J. Appl. Phys. 53 (1982) 2362.
[3] A. Sukiennicki, E. Della Torre, J. Appl. Phys. 55 (1984) 3739.
[4] Te-Ho Wu, J.C. Wu, Bing-Mau Chen, Han-Ping D. Shieh, J. Appl. Phys. 85 (8) (1999) 5980.
[5] Te-Ho Wu, J.C. Wu, Bing-Mau Chen, Han-Ping D. Shieh, J. Magn. Magn. Mater. 202 (1999) 62.
[6] S. Rinaldi, L. Pareti, J. Appl. Phys. 50 (1979) 7719.
[7] Te-Ho Wu, Hong Fu, R.A. Hajjar, T. Suzuki, M. Mansuripur, J. Appl. Phys. 73 (3) (1993) 1368.
[8] Wein-Kuen Hwang, Te-Ho, Han-Ping D. Shieh, J. Appl. Phys. 81 (11) (1997) 7437.